Support Information

Thermodynamic, electronic and optical properties of lead-free Hybrid double perovskite alloys of $MA_2B^+B^{3+}Br_6$ (B^+=Ag, K, Tl, B^{3+}=Bi, Sb, In)

Zhengwei Xu [a,b,*], Chang Li[a], Yexin Feng[c], Lei Wei[d], Lei Shen[b,*]

[a] Key Laboratory of Hunan Province on Information Photonics and Free space Optical Communications, School of physics and electrical sciences, Hunan Institute of Science and Technology, Yueyang 414006, People's Republic of China

[b] Department of Mechanical Engineering, National University of Singapore, Singapore 117575, Singapore

[c] Hunan Provincial Key Laboratory of Low-Dimensional Structural Physics and Devices, School of Physics and Electronics, Hunan University, Changsha 410082, China

[d] College of Mechanical Engineering, Hunan Institute of Science and Technology, Yueyang 414006, China;

Supplementary Text:

Here, we have considered two possible reference systems for $MA_2AgSbBr_6$ and MA_2KBiBr_6, one is the hypothetical structure of double perovskite phase and the other is the products of decomposition (BBr + B'Br$_3$). For the hypothetical $MA_2AgSbBr_6$ and MA_2KBiBr_6 double perovskite, which are the isostructural of $Cs_2AgSbBr_6$ and MA_2KBiCl_6, and crystallizes in $Fm\bar{3}m$ space group. The comparisons of total energies between double perovskite phase and BBr + B'Br$_3$ are shown in Table S1.

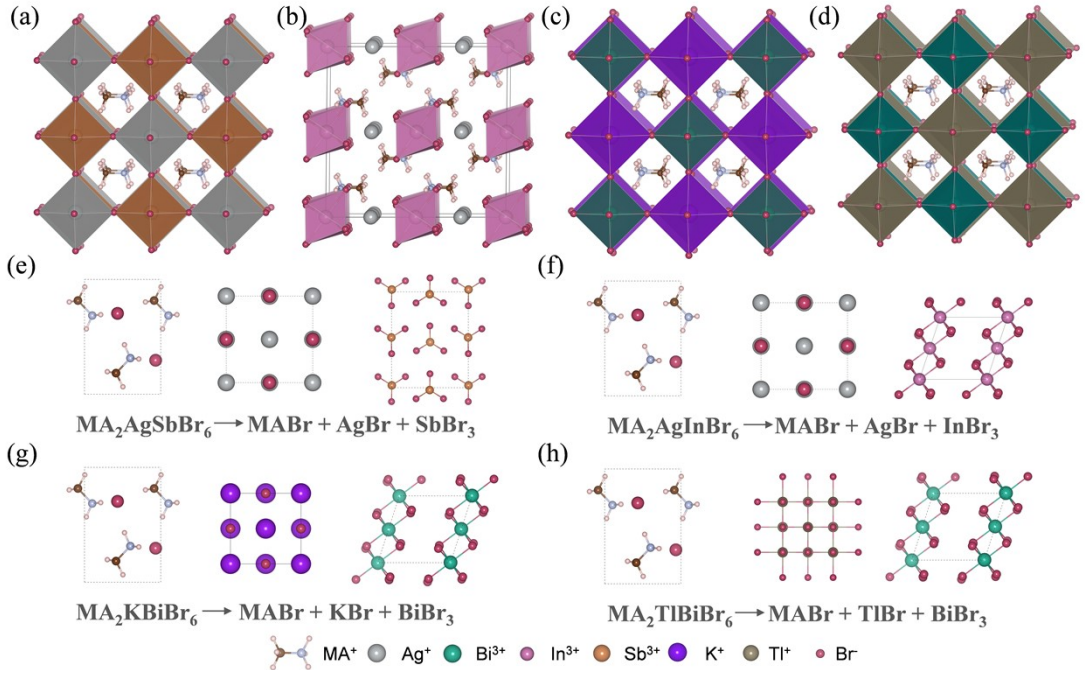

Fig. S1. Geometric structures of (a) hypothetical $MA_2AgSbBr_6$, (b) $MA_2AgInBr_6$, (c) hypothetical MA_2KBiBr_6, (d) $MA_2TlBiBr_6$. (e)-(h) Structures of MABr, BBr and B'Br$_3$, which represent the products of phase segregation $MA_2BB'Br_6$ → MABr + BBr + B'Br$_3$.

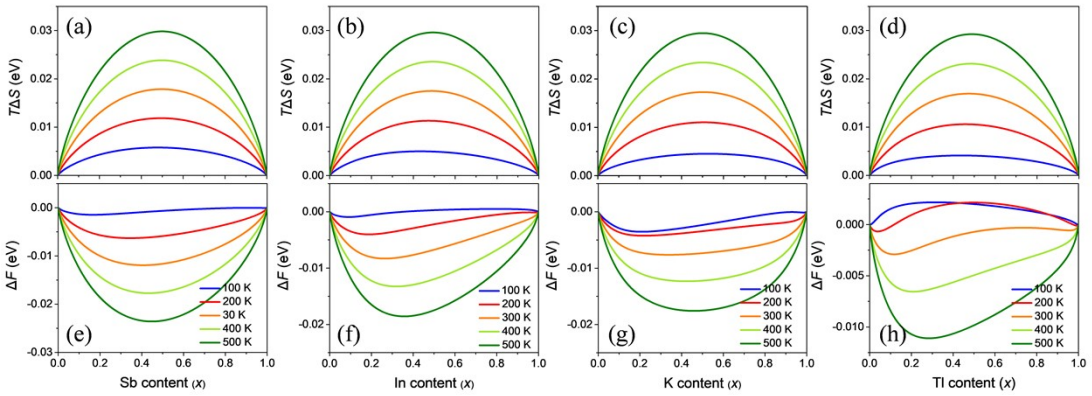

Fig. S2. Thermodynamic parameters as a function of the alloy composition and temperature for $MA_2AgSb_xBi_{1-x}Br_6$, $MA_2AgIn_xBi_{1-x}Br_6$, $MA_2K_xAg_{1-x}BiBr_6$ and

$MA_2Tl_xAg_{1-x}BiBr_6$ calculated within the GQCA at different temperature. Panels (a-d) are the mixed entropy ($T\Delta S$), and panels (e-h) are the Helmholtz free energy (ΔF).

TABLE S1 Main geometric parameters for the $MA_2BB'Br_6$.

Perovskite	a (Å)	b (Å)	c (Å)
$MA_2AgBiBr_6$	11.63	11.63	11.63
$MA_2AgSbBr_6$	11.71	11.71	11.71
$MA_2AgInBr_6$	7.63	7.63	7.05
MA_2KBiBr_6	11.45	11.45	11.45
$MA_2TlBiBr_6$	11.76	11.76	11.76

TABLE S2 Comparison of total energies between cubic phase and MABr+ BBr + $B'Br_3$ for $MA_2AgSbBr_6$ and MA_2KBiBr_6.

Compounds	Separate phase	Energy (eV)
$MA_2AgSbBr_6$	Cubic	**-102.61**
	MABr+AgBr+$SbBr_3$	-102.48
$MA_2AgInBr_6$	Cubic	**-101.84**
	MABr+AgBr+$SbBr_3$	101.52
MA_2KBiBr_6	Cubic	-102.92
	MABr+KBr+$BiBr_3$	**-102.99**
$MA_2TlBiBr_6$	Cubic	-102.85
	MABr+KBr+BiBr3	**-102.93**

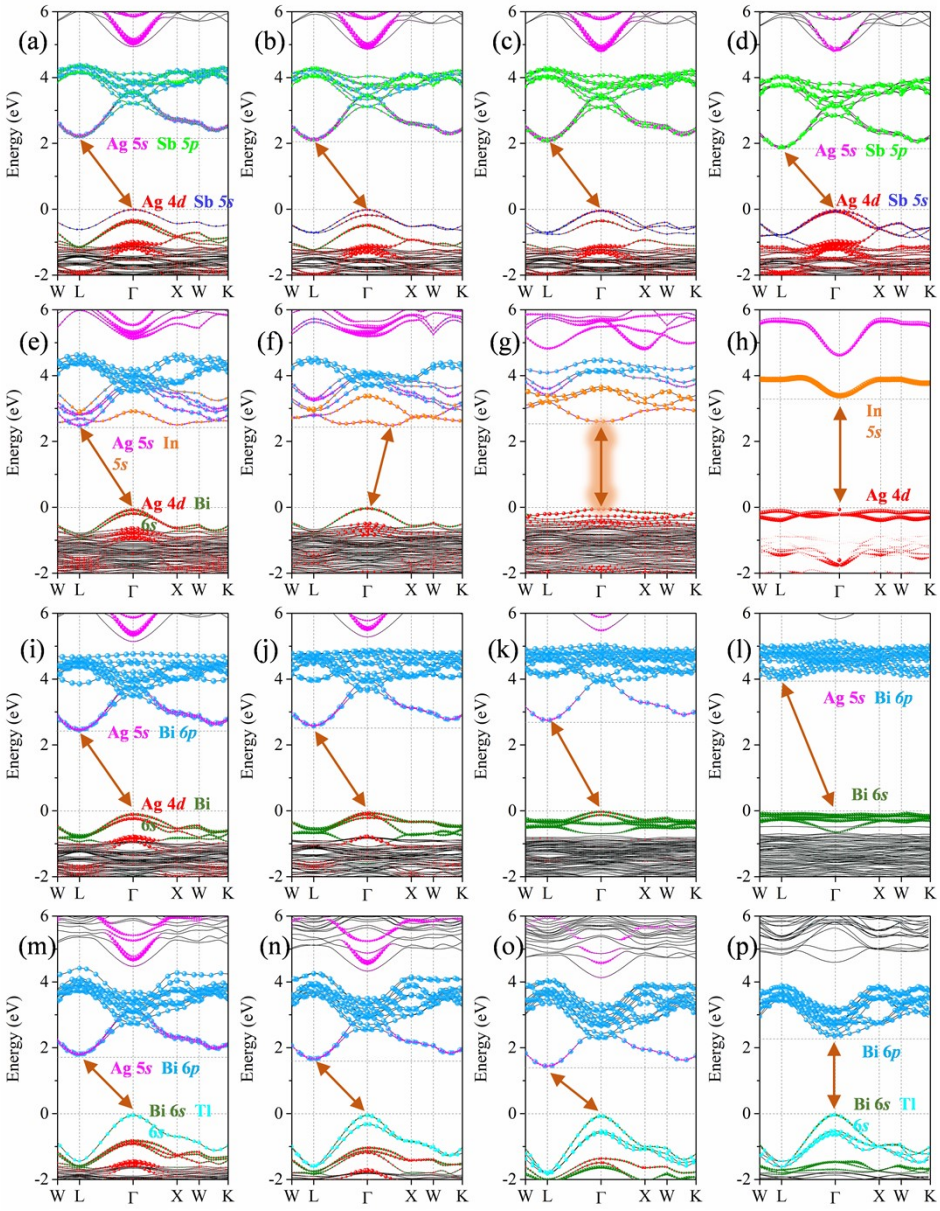

Fig. S3. HSE06 functional calculated band structure of various metal (a-d) Sb- (e-h) In- (i-l) K- (m-p) Tl-doped $MA_2AgBiBr_6$ alloy at concentrations 25%，50%，75%，100%，respectively.

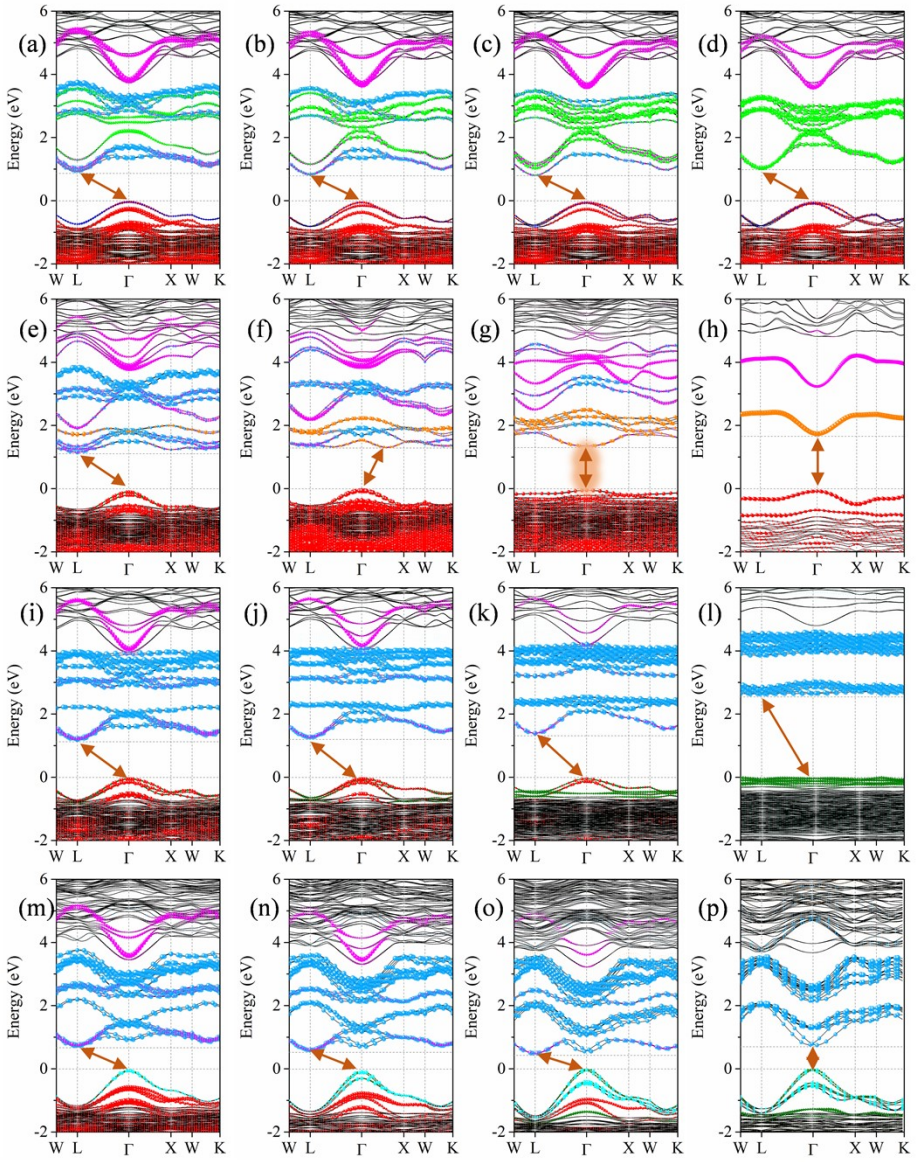

Fig. S4. PBE+SOC calculated band structure of various metal (a-d) Sb- (e-h) In- (i-l) K- (m-p) Tl-doped $MA_2AgBiBr_6$ alloy at concentrations 25%，50%，75%，100%, respectively.

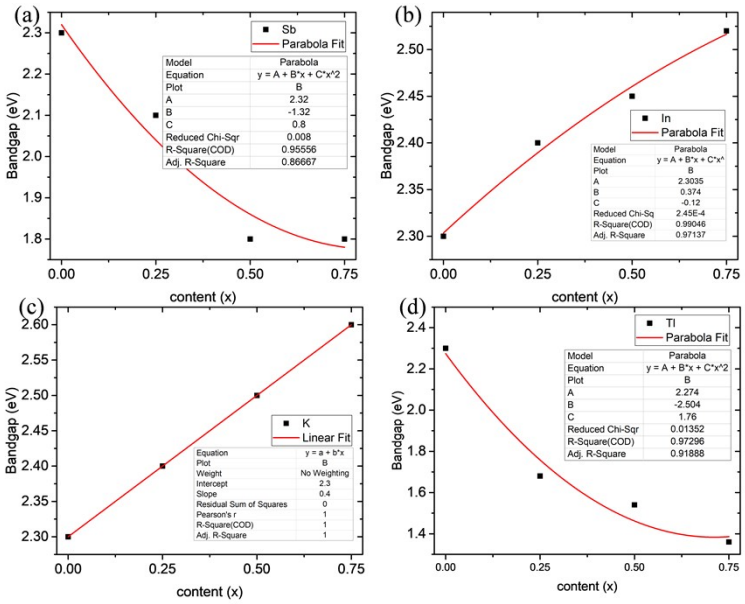

Fig. S5. The quadratic fit of the bandgaps as a function of doped composition (x).

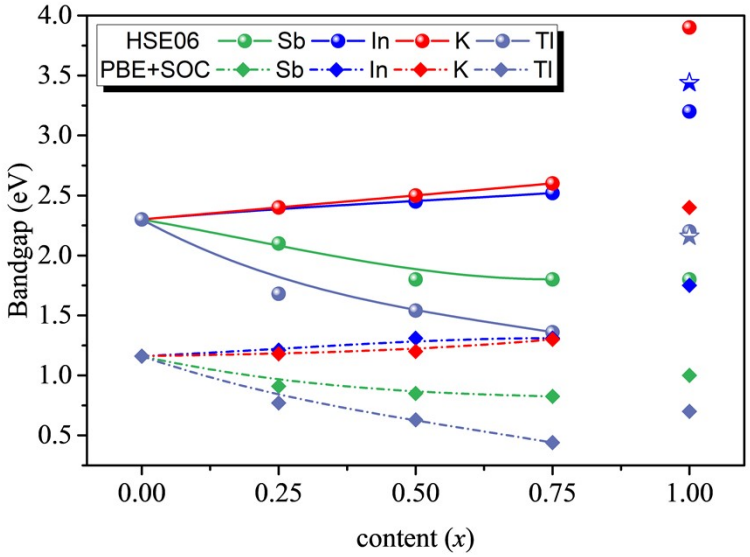

Fig. S6. Calculated band gaps of $MA_2AgIn_xBi_{1-x}Br_6$, $MA_2AgSb_xBi_{1-x}Br_6$, $MA_2K_xAg_{1-x}BiBr_6$, and $MA_2Tl_xAg_{1-x}BiBr_6$ as a function of doping content by HSE06 and PBE+SOC. The star symbol represents experimental values.

TABLE S3 Calculated absorption coefficients α (10^5 cm^{-1}) at selected photon energies for $MAPbI_3$ and the studied double perovskite alloys.

Photon Energy (eV)	Absorption Coefficient α (10^5 cm^{-1})					
	$MAPbI_3$	$MA_2AgBiBr_6$	$Sb_{0.75}$ doped	$In_{0.75}$ doped	$K_{0.75}$ doped	$Tl_{0.75}$doped
2.0	0.50	0.23	1.58	0.71	0.09	1.24
2.5	2.40	1.80	2.24	1.47	0.78	3.36
3.0	5.04	3.86	3.83	2.23	1.63	4.30
3.5	6.96	6.74	5.61	3.16	1.85	4.64
4.0	6.78	6.30	6.14	3.54	4.56	5.60

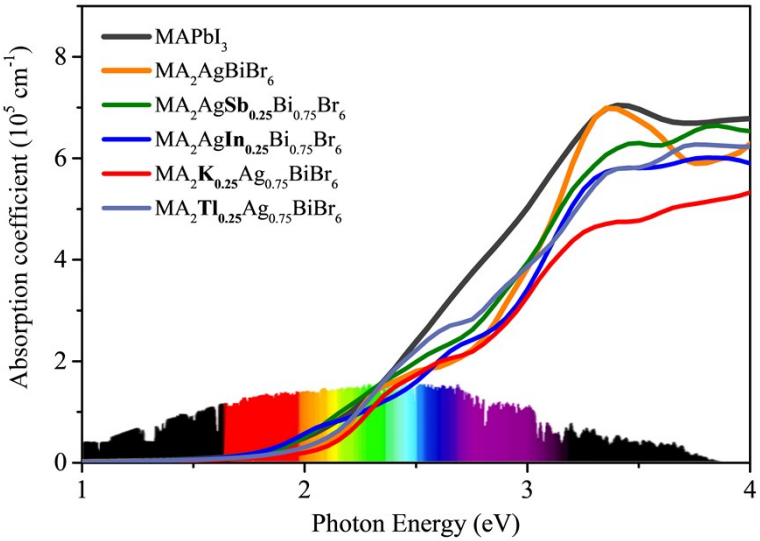

Fig. S7. Calculated optical absorption spectra of $MA_2AgBiBr_6$-based alloys with doping content of x=25%. For comparison, the spectra of $MAPbI_3$ is also shown. The standard AM1.5G solar spectrum is displayed at the bottom as a reference, with colors ranging from red to purple denoting the visible light region.

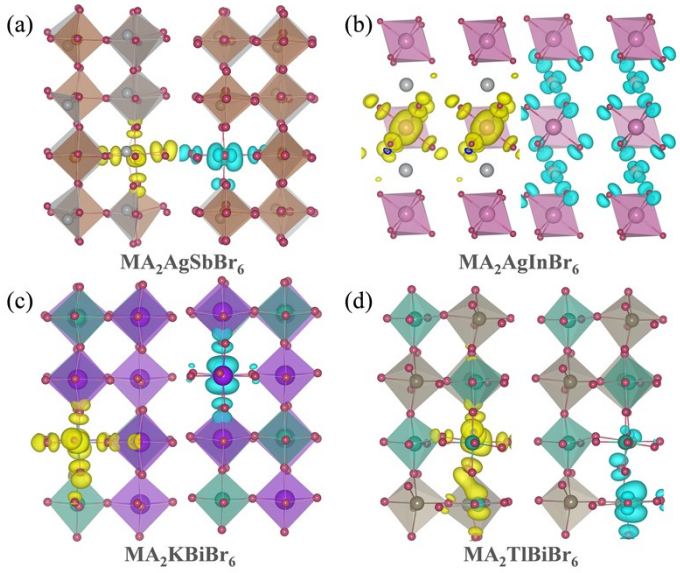

Fig. S8. Partial charge density contours of the hole (yellow) and electron states (cyan) for the exciton in pristine (a) $MA_2AgSbBr_6$, (b) $MA_2AgInBr_6$, (c) MA_2KBiBr_6, and (d) $MA_2TlBiBr_6$.Only the inorganic framework is shown, and molecular cations have been omitted.

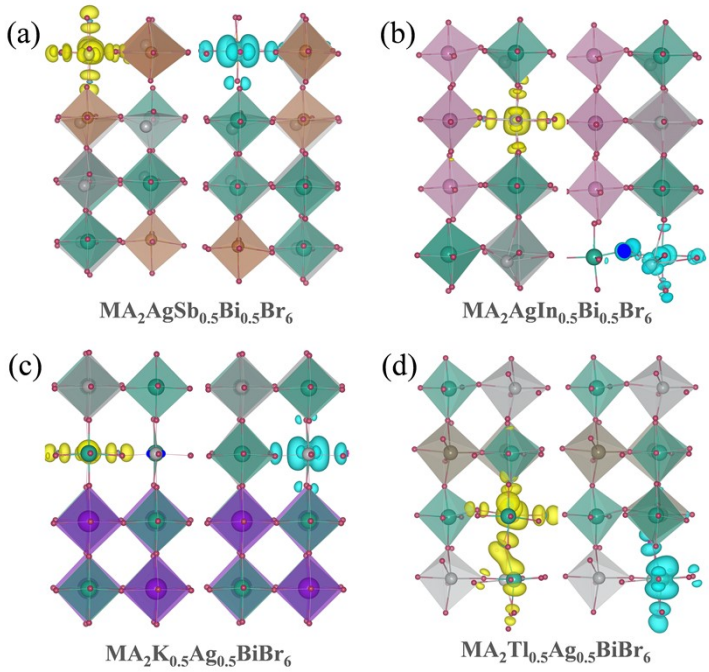

Fig. S9. Partial charge density contours of the hole (yellow) and electron states (cyan) for the exciton in (a) $MA_2AgSb_{0.5}Bi_{0.5}Br_6$, (b) $MA_2AgIn_{0.5}Bi_{0.5}Br_6$, (c) $MA_2K_{0.5}Ag_{0.5}BiBr_6$, and (d) $MA_2Tl_{0.5}Ag_{0.5}BiBr_6$. Only the inorganic framework is shown, and molecular cations have been omitted.